TU Delft

Delft University of Technology

Buck-Boost Flying Capacitor DC-DC Converter for Electric Vehicle Charging Stations

Pesantez, D.; Rodriguez, F.; Renaudineau, H.; Rivera, S.; Kouro, S.

DOI
10.1109/CPE-POWERENG58103.2023.10227461

Publication date
2023

Document Version
Final published version

Published in
CPE-POWERENG 2023 - 17th IEEE International Conference on Compatibility, Power Electronics and Power Engineering

Citation (APA)
Pesantez, D., Rodriguez, F., Renaudineau, H., Rivera, S., & Kouro, S. (2023). Buck-Boost Flying Capacitor DC-DC Converter for Electric Vehicle Charging Stations. In *CPE-POWERENG 2023 - 17th IEEE International Conference on Compatibility, Power Electronics and Power Engineering* (CPE-POWERENG 2023 - 17th IEEE International Conference on Compatibility, Power Electronics and Power Engineering). IEEE. https://doi.org/10.1109/CPE-POWERENG58103.2023.10227461

Important note
To cite this publication, please use the final published version (if applicable).
Please check the document version above.

Copyright
Other than for strictly personal use, it is not permitted to download, forward or distribute the text or part of it, without the consent of the author(s) and/or copyright holder(s), unless the work is under an open content license such as Creative Commons.

Takedown policy
Please contact us and provide details if you believe this document breaches copyrights.
We will remove access to the work immediately and investigate your claim.

This work is downloaded from Delft University of Technology.
For technical reasons the number of authors shown on this cover page is limited to a maximum of 10.

Green Open Access added to TU Delft Institutional Repository

'You share, we take care!' - Taverne project

https://www.openaccess.nl/en/you-share-we-take-care

Otherwise as indicated in the copyright section: the publisher is the copyright holder of this work and the author uses the Dutch legislation to make this work public.

2023 IEEE 17th International Conference on Compatibility, Power Electronics and Power Engineering (CPE-POWERENG) | 979-8-3503-0004-8/23/$31.00 ©2023 IEEE | DOI: 10.1109/CPE-POWERENG58103.2023.10227461

Buck-Boost Flying Capacitor DC-DC Converter for Electric Vehicle Charging Stations

D. Pesantez
Electronics Engineering Department
Univ. Tecnica Federico Santa Maria
Valparaiso, Chile
alvaro.pesantez@sansano.usm.cl

F. Rodriguez
Electronics Engineering Department
Univ. Tecnica Federico Santa Maria
Valparaiso, Chile
francisco.rodriguezh@sansano.usm.cl

H.Renaudineau
Electronics Engineering Department
Univ. Tecnica Federico Santa Maria
Valparaiso, Chile
hugues.renaudineau@usm.cl

S. Rivera
Department of Electrical Sustainable Energy
Delft University of Technology
Delft, The Netherlands
s.rivera.i@ieee.org

S. Kouro
Electronics Engineering Department
Univ. Tecnica Federico Santa Maria
Valparaiso, Chile
Department of Electronic Engineering
Universidad de Sevilla
Sevilla, España
samir.kouro@ieee.org

***Abstract*—This paper proposes a new buck-boost flying-capacitor (FC) converter for the DC-DC stage of an Electric Vehicle (EV) fast charging station. The proposed converter is capable of delivering a wide output range of voltage to charge different battery configurations. The converter has two modes of operation, buck and boost. Thanks to this feature, the proposed converter allows higher efficiency and a wide operating range. The proposed converter is capable of supplying a voltage range from 200 V to 1000 V at its output, which shows the feasibility of occupying the converter inside a charging station that allows charging 400 V and 800 V battery systems. The average efficiency reported is over 97%. It is concluded that the proposed buck-boost FC converter is suitable for modern wide-output EV fast charging applications.**

***Index Terms*—Electric Vehicles, Fast Charging, Flying-Capacitor.**

I. Introduction

In recent years, the development of electric vehicles has gained significant importance within the automotive industry due to the imminent change expected from the old internal combustion systems to fully electric systems [1].

However, the rapid development of electric vehicles has brought important challenges, mainly regarding the battery [2]. Lifetime, charging time, and energy density, among others, are battery characteristics that define the behavior of the EV. Some of these features are directly related to the battery charger, so the development of these must go hand in hand with the advancement of battery technologies.

In the last years, battery capacity has been pushed up to the 60-120 kWh range. This improvement has imposed substantial challenges on battery chargers, and available charging rates [3], [4]. With current fast charging technologies rated at 50 kW, it takes between 35 and 120 minutes to recharge the battery [5]. However, by increasing the charging power level to 150 kW, this can effectively reduce the charging times.

Over the past decade, most EVs have used battery configurations in the range of 150 to 450 V; this voltage configuration is often called the 400 V system. In order to offer an improvement in the power rating and charging times, 800 V DC systems have been proposed [6]. Therefore, the two biggest challenges for new EV battery chargers are achieving high charging power and high efficiency, providing a wide output voltage range so that 400V and 800V systems can coexist.

Several DC-DC converters have been proposed to cover the needs of new charging stations. For example, Tesla Supercharger V2 comprises a phase-shift full bridge DC-DC converter. Tesla Supercharger is built in a modular way and can charge a battery up to 150 kW, with a reported maximum efficiency of 92% [7]. In [8] a cascaded H-bridge converter is employed to interface the medium voltage grid, while a dual active bridge converter with galvanic isolation serves as a wide output interface with EVs. Another wide output solution, based on a reconfigurable LLC resonant DC-DC converter, is presented in [9].

On the other hand, there are solutions without galvanic isolation; for instance, in [10], [11], [12], topologies based on the partial power converter concept have been proposed. A non-isolated topology for wide output fast charging stations is proposed in [13]; a full bridge topology is connected through an impedance network, comprised of an LCC configuration, to an output diode bridge, producing a wide output voltage in the output.

After presenting existing buck-boost FC converters in section II-A, this paper proposed a new buck-boost FC converter in section II-B. Control of the converter is explained in section II-C. Simulation results and the main conclusions obtained are shown in sections III and IV.

Authorized licensed use limited to: TU Delft Library. Downloaded on September 29,2023 at 08:49:05 UTC from IEEE Xplore. Restrictions apply.

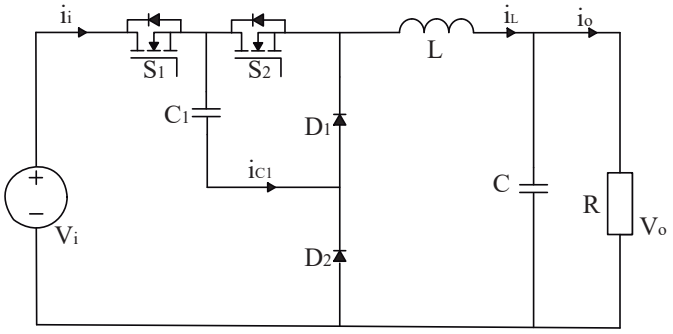

Fig. 1: Flying-capacitor buck converter

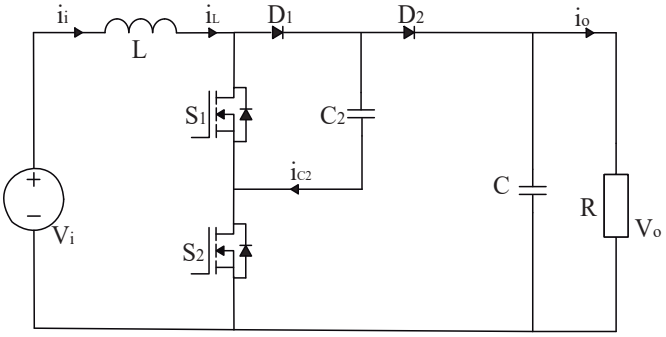

Fig. 2: Flying-capacitor boost converter

II. Proposed buck-boost FC converter

A. Buck and boost FC converters overview

In the study of high voltage and high power applications, flying-capacitor converters were introduced in [14]. Based on this principle, several topologies have been developed for different applications [15], one of which corresponds to the flying-capacitor DC-DC buck converter (FCBC). Among the main advantages of FCBC over traditional buck converters are the lowest switch voltage stress, smaller passive components size, and a higher power density [16].

A detailed study of a FCBC is presented in [17]; this converter consists of four semiconductors, two MOSFETs, and two diodes, as shown in Fig. 1.

The linear characteristic of the converter, shown in Eq. (1), allows having an output voltage proportional to the duty cycle d_{bu} of the S_1 switch. The two pairs of semiconductors work in a complementary way, i.e., if S_1 is ON, D_2 is OFF, and if S_2 is ON, D_1 is OFF. S_1 and S_2 operate with classical bipolar PWM commutation.

$$V_o = d_{bu} \cdot V_{in} \tag{1}$$

Otherwise, there are boost FC topologies for high energy density applications [18], [19]. An analysis of the operation and control of the three-level flying-capacitor boost converter, shown in Fig. 2, is presented in [20]. Similarly to the operation of the FCBC, the two pairs of semiconductors work in a complementary way. The transfers function of the converter is a function of the duty cycle d_{bo} of S_1 switch, as it is shown in Eq. (2).

$$V_i = (1 - d_{bo}) \cdot V_o \tag{2}$$

B. Proposed buck-boost FC converter

The present work proposes a new buck-boost FC converter, depicted in Fig. 3. Based on the converters presented in the previous section, the proposed converter joins the buck and the boost converters through a single inductor L. The main advantage of this topology is the wide output voltage range and high conversion efficiency.

Some buck-boost converter configurations designed for EV charging applications can be found in the literature. However, these show designs for single voltage values [21]. On the other hand, buck-boost topologies can be found adapted to offer a greater voltage range. However, these imply a more significant number of components and the most complicated control strategy [22].

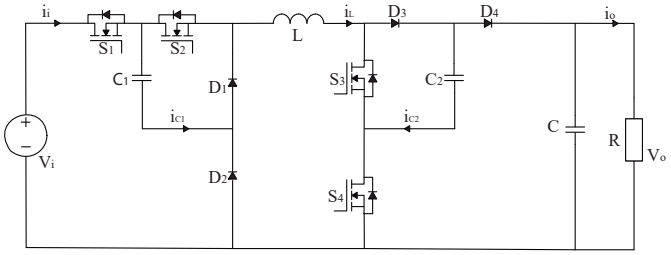

Fig. 3: Proposed buck-boost flying-capacitor converter

The operation of the converter can be analyzed in two modes, buck mode, and boost mode. For buck mode, the MOSFETs S_3 and S_4 stay off, while diodes D_3 and D_4 are on. The pair of semiconductors S_1 and D_1 operates in a complementary way with the pair S_2 and D_2. For boost mode, the MOSFETs S_1 and S_3 always stay on to allow the current flow through the inductor L. Semiconductors S_3, S_2, D_3, and D_4 operate analogously to the buck mode. The output voltage of the converter is a function of the duty cycle of the PWM signals used to drive the MOSFETs; according to the operation mode, it defines D_d as the duty cycle of S_1 and S_2 switches for buck mode and, D_u as the duty cycle of S_3 and S_4 switches for boost mode, as shown in Eq. (3) and Eq. (4).

$$V_o = D_d \cdot V_i, \quad 0 < D_d < 1 \tag{3}$$

$$V_o = \frac{1}{1 - D_u} \cdot V_i, \quad 0 < D_u < 1 \tag{4}$$

The eight operation states derived from the converter are detailed in Table I, where it can be appreciated the equivalent circuit operation, and state variables equations for each respective state of operation.

Authorized licensed use limited to: TU Delft Library. Downloaded on September 29,2023 at 08:49:05 UTC from IEEE Xplore. Restrictions apply.

TABLE I: Proposed converter operation and state variable modelling

Mode		Circuit operation	State variable equations
Buck	State I	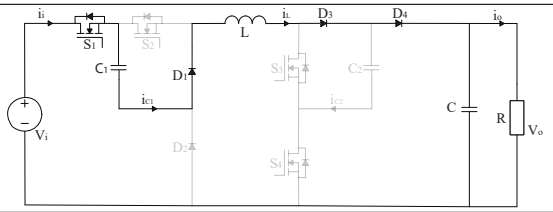	$\begin{cases} C_1\frac{dV_{C_1}(t)}{dt} = i_L(t) \\ C_2\frac{dV_{C_2}(t)}{dt} = 0 \\ L\frac{di_L(t)}{dt} = V_i - V_{C_1}(t) - V_o(t) \\ C\frac{dV_C(t)}{dt} = i_L(t) - i_o(t) \end{cases}$
	State II	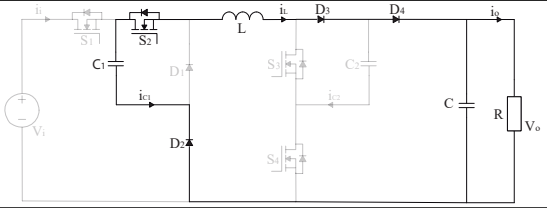	$\begin{cases} C_1\frac{dV_{C_1}(t)}{dt} = -i_L(t) \\ C_2\frac{dV_{C_2}(t)}{dt} = 0 \\ L\frac{di_L(t)}{dt} = V_{C_1}(t) - V_o(t) \\ C\frac{dV_C(t)}{dt} = i_L(t) - i_o(t) \end{cases}$
	State III	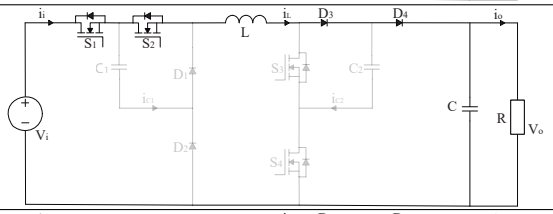	$\begin{cases} C_1\frac{dV_{C_1}(t)}{dt} = 0 \\ C_2\frac{dV_{C_2}(t)}{dt} = 0 \\ L\frac{di_L(t)}{dt} = V_i - V_o(t) \\ C\frac{dV_C(t)}{dt} = i_L(t) - i_o(t) \end{cases}$
	State IV	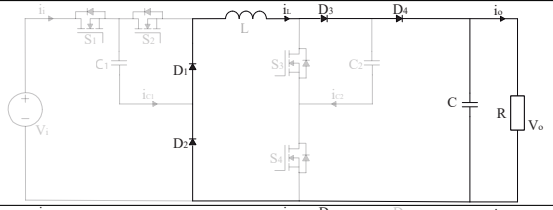	$\begin{cases} C_1\frac{dV_{C_1}(t)}{dt} = 0 \\ C_2\frac{dV_{C_2}(t)}{dt} = 0 \\ L\frac{di_L(t)}{dt} = -V_o(t) \\ C\frac{dV_C(t)}{dt} = i_L(t) - i_o(t) \end{cases}$
Boost	State V	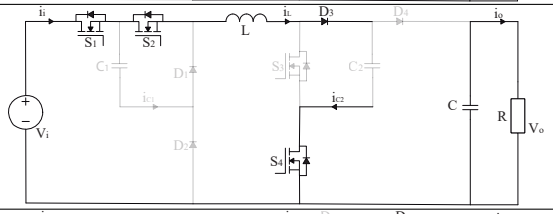	$\begin{cases} L\frac{di_L(t)}{dt} = V_i - V_{C_1}(t) \\ C_1\frac{dV_{C_1}(t)}{dt} = 0 \\ C_2\frac{dV_{C_2}(t)}{dt} = i_L(t) \\ C\frac{dV_C(t)}{dt} = -i_o(t) \end{cases}$
	State VI	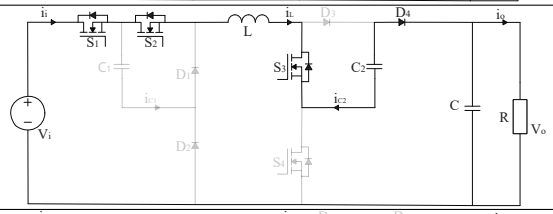	$\begin{cases} L\frac{di_L(t)}{dt} = V_i + V_{C_2}(t) - V_o(t) \\ C_1\frac{dV_{C_1}(t)}{dt} = 0 \\ C_2\frac{dV_{C_2}(t)}{dt} = -i_L(t) \\ C\frac{dV_C(t)}{dt} = i_L(t) - i_o(t) \end{cases}$
	State VII	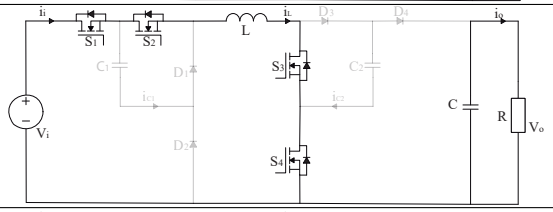	$\begin{cases} L\frac{di_L(t)}{dt} = V_i \\ C_1\frac{dV_{C_1}(t)}{dt} = 0 \\ C_2\frac{dV_{C_2}(t)}{dt} = 0 \\ C\frac{dV_C(t)}{dt} = -i_o(t) \end{cases}$
	State VIII	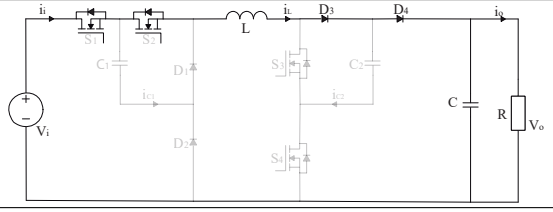	$\begin{cases} L\frac{di_L(t)}{dt} = -V_o(t) \\ C_1\frac{dV_{C_1}(t)}{dt} = 0 \\ C_2\frac{dV_{C_2}(t)}{dt} = 0 \\ C\frac{dV_C(t)}{dt} = i_L(t) - i_o(t) \end{cases}$

Authorized licensed use limited to: TU Delft Library. Downloaded on September 29,2023 at 08:49:05 UTC from IEEE Xplore. Restrictions apply.

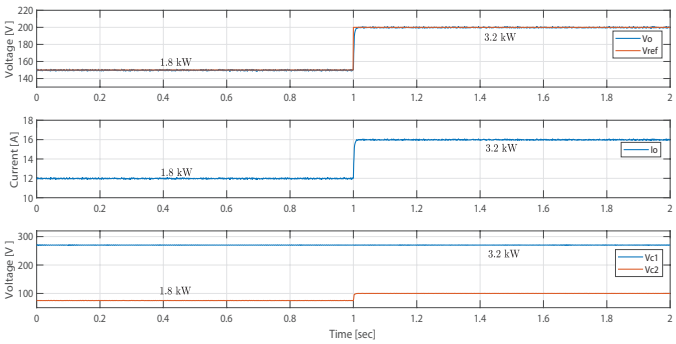

Fig. 4: Simulation results of the proposed converter in buck mode

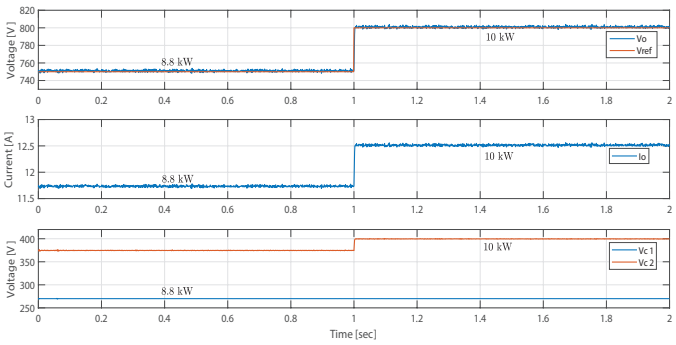

Fig. 5: Simulation results of the proposed converter in boost mode

C. Converter control

The control of the proposed converter is based on a cascade control loop using traditional PI controllers. For the correct operation of the converter, PI controller parameters are dimensioned for buck and boost operation modes, as shown in Fig. 6.

The output voltage of the converter is controlled by controlling the inductor current L. According to the charging algorithm, the BMS defines the reference signals for those control loops, as shown in Fig. 6. For this work, the constant current and constant voltage algorithm (CC-CV) is used [23], and the reference signal changes according to the state of charge of the battery. When the charging process starts, the BMS establishes the current reference so that the charging station can operate at its nominal current. This reference is held until the battery reaches its rated voltage value; then, the battery determines how much current it must absorb to complete its charge. Therefore, from this moment, the current controller reference changes the signal of the output of the external controller, allowing it to keep the battery voltage constant at its nominal value. Each of the capacitors of the proposed converter should be appropriately maintained according to a voltage reference. For this, two independent PI controllers are used. The reference for each capacitor, C1, and C2, equals $Vi/2$ and $Vo/2$, respectively [17], [18].

The output signal D corresponds to the d_{bu} and d_{bo} signals from the PI controllers for each operation mode, depending on the inverter operating status, shown in Fig. 6.

Signals D and U_{cx}, allow obtaining the switching signals of each of the MOSFETs through a PWM modulation block.

III. Simulation Results

The first result corresponds to the voltage behavior of the capacitors C_1 and C_2, for the buck and boost operation modes. Fig. 4 shows the simulation results for the buck mode. Considering an input voltage of 540 V and an initial power of 1.8 kW. At the time $t = 1s$, the converter faces a change in the output power to 3.2 kW. The results show that the system behaves as expected. At the beginning of the simulation, the output voltage is equal to 150 V. After the power change at $t = 1s$, the output voltage increase to 200 V, and it is observed that the converter output voltage follows its reference before and after the increase in output power. The voltage on the capacitor C_1 is always regulated at 270 V, a value corresponding to half the input voltage V_i, while the voltage on the capacitor C_2 is maintained at the half the output voltage V_o. For the boost mode, considering the same input voltage 540 V, the correct system behavior is shown in Fig. 5. Initially, the converter operates at an output power of 8.8 kW, with an output voltage of 750 V, at the time $t = 1s$, the converter faces a change in the output power to 10 kW. After the power change, the output voltage increase to 800 V, it is observed that the capacitors C_1 and C_2 maintain the same behavior as for the buck mode.

A second simulation is performed with a 4.5 kWh Li-ion battery model used to simulate the proposed converter as part of a charging station for both systems 400 V, and 800 V. Table II shows the parameters used to simulate the DC-DC converter as part of the fast-charging station.

Figures 7 and 8 show the proposed converter operation for 400 V and 800 V systems. The behavior of the charging system is shown according to the CCCV algorithm. It consists of two stages. The first corresponds to the constant current mode; in this stage, a fixed current value is supplied to the battery, controlled by the battery management system (BMS) until it reaches the desired level of its state of charge

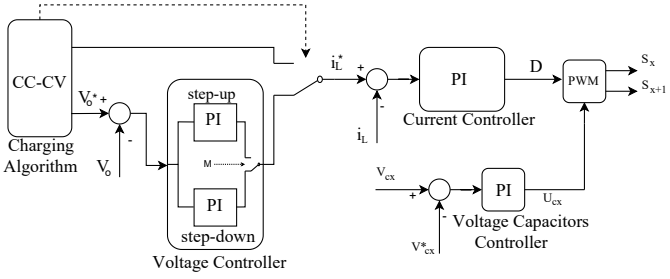

Fig. 6: General control scheme

Authorized licensed use limited to: TU Delft Library. Downloaded on September 29,2023 at 08:49:05 UTC from IEEE Xplore. Restrictions apply.

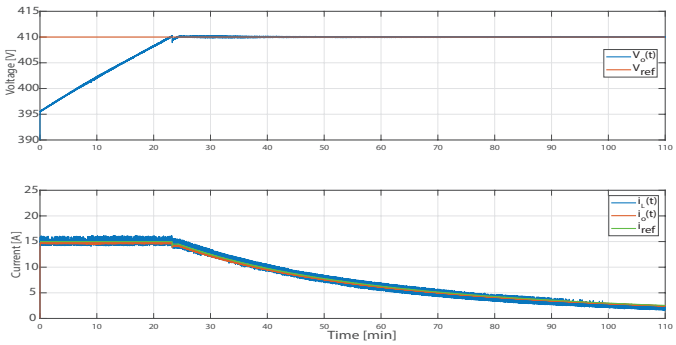

Fig. 7: Simulation results of the proposed converter for the charging of a 400V battery

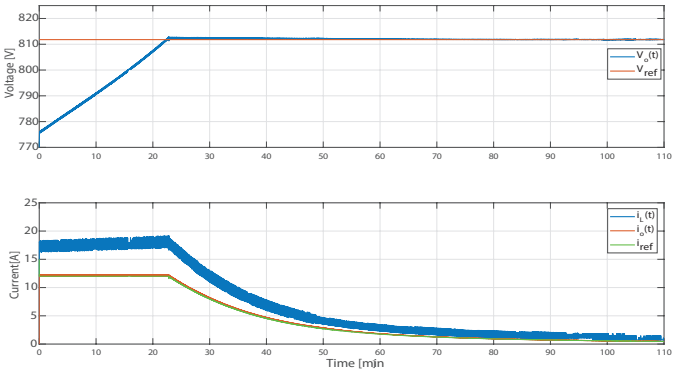

Fig. 8: Simulation results of the proposed converter for the charging of a 800V battery

(SoC); generally, this value is around 90%. The constant voltage stage is responsible for getting the battery to 100% SoC without risk. In this stage, a constant voltage is applied between the battery terminals equal to the system nominal voltage of the battery. As the battery reaches the desired voltage level, the current gradually decreases to a minimum value.

TABLE II: Simulation Parameters

Parameter	Values
Input Voltage	540 V
Inductor	397 μH
C1	274 μF
C2	126 μF
Switching Frequency	25 kHz

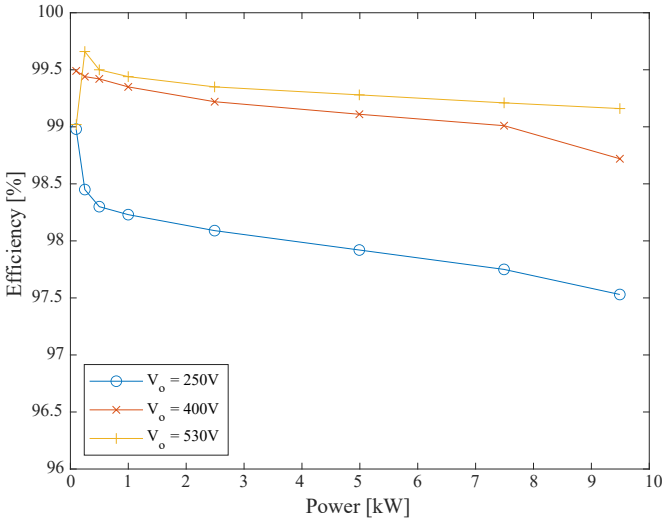

Fig. 9: Estimated efficiency in buck mode

For the 400 V system, Fig. 7 shows the converter output voltage and output current, both with their respective reference signals. It is observed how the signals follow their references according to the loading algorithm. The ripple in the inductor current i_L shows a maximum value of 13%; however, the ripple in the output current i_o reaches a maximum value of 1.7%. For the 800 V battery system, Fig. 8 shows the output current and voltage and references signals of the converter. The ripple in the inductor current i_L shows a maximum value of 12.1%; however, the ripple in the output current i_o reaches a maximum value of 2%. These ripple values at the converter output make this a good proposal for use within a charging station with a wide voltage output range. The voltage variation is much lower in 400V system due to the different capacity (Ah) of the battery for the same (kWh) pack.

Using the component PLECS thermal model, a simulation of the efficiency of the proposed converter is performed. The MOSFET models MSC025SMA120B and diodes MSC050SDA170B developed by MICROCHIP were employed. The efficiency of the converter is shown for the two modes of operation. Figure 9 shows the efficiency of the converter in the buck mode. It is observed that the efficiency is higher when the output voltage is close to the input voltage, with a maximum of 99.6%. Efficiency reduces for values more proximate to the 200V limit with a reported minimum efficiency of 97.5% for a power of 9.6 kW. Figure 10 shows the same efficiency analysis for the boost mode, as in the reducer case, the efficiency reports a higher value for values close to the input voltage, with a maximum of 99.6%, and the minimum is given for values further away from the input voltage, a minimum of 96.6% is reported for a converter power of 9.6 kW. Although efficiency decreases for higher power values, the proposed converter still maintains a high value compared to existing converters on the market.

IV. Conclusion

This work proposed a new buck-boost flying capacitor DC-DC converter for wide voltage output EV battery charging stations. The proposed converter comprises four semiconductors, which allow operating in buck or boost mode with the

Authorized licensed use limited to: TU Delft Library. Downloaded on September 29,2023 at 08:49:05 UTC from IEEE Xplore. Restrictions apply.

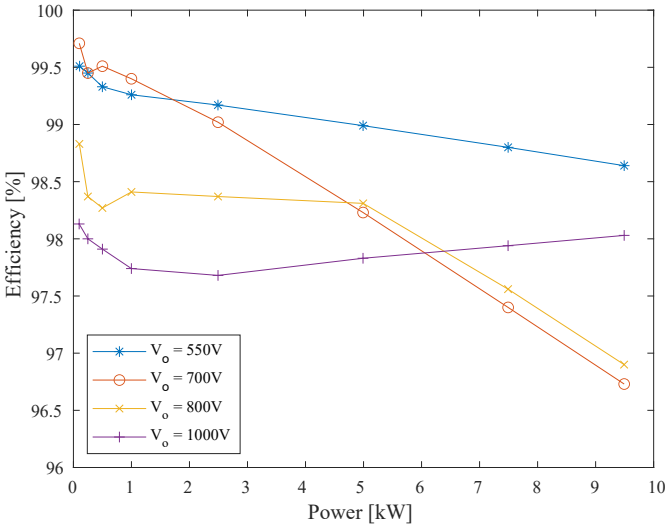

Fig. 10: Estimated efficiency in boost mode

correct modulation. The theoretical analysis shows some of the advantages of using flying capacitor converters. The simulation results show the correct behavior of the proposed converter as a battery charger. Simulations were carried out for the two systems with different voltage level, where their control were validated for the proposed power converter. It can be observed that the converter presents the necessary characteristics for battery charging, such as its wide voltage range, between 200V to 1000V, and the minimal ripple in the output current. Finally, the estimated efficiency of the proposed converter shows that the proposed solution allows high efficiency over a wider power range, especially for output voltages close to the input value. It is then concluded that the proposed solution is suitable for EV fast charging applications.

Acknowledgment

The authors gratefully acknowledge the financial support provided by ANID/Fondecyt 1221741, AC3E (ANID/BASAL/FB0008), SERC (ANID/FONDAP/15110019) and ANID/FONDEQUIP/EQM180215, ANID-Subdirección de Capital Humano/Doctorado Nacional/2022-21221405, Dirección de Postgrado y Programas/ Universidad Técnica Federico Santa María.

References

[1] IEA, "Global EV Outlook 2021 - Accelerating ambitions despite the pandemic," *Global EV Outlook 2021*, p. 101, 2021. [Online]. Available: https://iea.blob.core.windows.net/assets/ed5f4484-f556-4110-8c5c-4ede8bcba637/GlobalEVOutlook2021.pdf

[2] Z. P. Cano, D. Banham, S. Ye, A. Hintennach, J. Lu, M. Fowler, and Z. Chen, "Batteries and fuel cells for emerging electric vehicle markets," *Nature Energy*, vol. 3, no. 4, pp. 279–289, 2018.

[3] S. Rivera, S. Kouro, S. Vazquez, S. M. Goetz, R. Lizana, and E. Romero-Cadaval, "Electric Vehicle Charging Infrastructure: From Grid to Battery," *IEEE Industrial Electronics Magazine*, vol. 15, no. 2, pp. 37–51, 2021.

[4] S. Rivera, S. M. Goetz, S. Kouro, P. W. Lehn, M. Pathmanathan, P. Bauer, and R. A. Mastromauro, "Charging Infrastructure and Grid Integration for Electromobility," *Proceedings of the IEEE*, vol. 111, no. 4, pp. 371–396, 2023.

[5] I. Aghabali, J. Bauman, P. J. Kollmeyer, Y. Wang, B. Bilgin, and A. Emadi, "800-V Electric Vehicle Powertrains: Review and Analysis of Benefits, Challenges, and Future Trends," *IEEE Transactions on Transportation Electrification*, vol. 7, no. 3, pp. 927–948, 2021.

[6] C. Jung, "Power Up with 800-V Systems," *IEEE Electrification Magazine*, vol. 5, no. 1, pp. 53–58, 2017.

[7] J.-P. Krauer, "Charging Efficiency Using Variable Isolation," *US Patent 9.225,197 B2*, vol. 2, no. 12, 2015. [Online]. Available: https://patents.google.com/patent/US9225197B2/en

[8] V. M. Iyer, S. Gulur, G. Gohil, and S. Bhattacharya, "An approach towards extreme fast charging station power delivery for electric vehicles with partial power processing," *IEEE Transactions on Industrial Electronics*, vol. 67, no. 10, pp. 8076–8087, 2020.

[9] E. V. De Souza and M. L. Heldwein, "Reconfigurable Resonant Converter with Wide Output Voltage Range for DC Fast Chargers," *2021 Brazilian Power Electronics Conference, COBEP 2021*, 2021.

[10] J. Anzola, I. Aizpuru, and A. Arruti, "Non-Isolated Partial Power Converter for Electric Vehicle Fast Charging Stations," *2020 IEEE 11th International Symposium on Power Electronics for Distributed Generation Systems, PEDG 2020*, pp. 18–22, 2020.

[11] S. Rivera, J. Rojas, S. Kouro, P. W. Lehn, R. Lizana, H. Renaudineau, and T. Dragicevic, "Partial-Power Converter Topology of Type II for Efficient Electric Vehicle Fast Charging," *IEEE Journal of Emerging and Selected Topics in Power Electronics*, vol. 10, no. 6, pp. 7839–7848, 2021.

[12] S. Rivera, D. Pesantez, S. Kouro, and P. W. Lehn, "Pseudo-Partial-Power Converter without High Frequency Transformer for Electric Vehicle Fast Charging Stations," *2018 IEEE Energy Conversion Congress and Exposition, ECCE 2018*, pp. 1208–1213, 2018.

[13] D. Pesantez, H. Renaudineau, S. Rivera, and S. Kouro, "Transformerless Partial Power Converter for Electric Vehicle Fast Charging Stations," *2022 IEEE Energy Conversion Congress and Exposition, ECCE 2022*, pp. 1–6, 2022.

[14] T. A. Meynard and H. Foch, "Multi-level conversion: High voltage choppers and voltage-source inverters," *PESC Record - IEEE Annual Power Electronics Specialists Conference*, pp. 397–403, 1992.

[15] H. Akagi, "Multilevel Converters: Fundamental Circuits and Systems," *Proceedings of the IEEE*, vol. 105, no. 11, pp. 2048–2065, 2017.

[16] T.-l. B. Dc and D. C. Converters, "Second-Order Sliding-Mode Controlled," *IEEE Transactions on Industrial Electronics Electronics*, vol. 65, no. 1, pp. 898–906, 2018.

[17] A. El Aroudi, B. G. M. Robert, A. Cid-Pastor, and L. Martínez-Salamero, "Modeling and design rules of a two-cell buck converter under a digital PWM controller," *IEEE Transactions on Power Electronics*, vol. 23, no. 2, pp. 859–870, 2008.

[18] Z. Liao, Y. Lei, and R. C. Pilawa-Podgurski, "Analysis and Design of a High Power Density Flying-Capacitor Multilevel Boost Converter for High Step-Up Conversion," *IEEE Transactions on Power Electronics*, vol. 34, no. 5, pp. 4087–4099, may 2019.

[19] W. C. Liu, P. H. Ng, and R. Pilawa-Podgurski, "A Three-Level Boost Converter with Full-Range Auto-Capacitor-Compensation Pulse Frequency Modulation," *IEEE Journal of Solid-State Circuits*, vol. 55, no. 3, pp. 744–755, mar 2020.

[20] H. C. Chen, C. Y. Lu, W. H. Lien, and T. H. Chen, "Active Capacitor Voltage Balancing Control for Three-Level Flying Capacitor Boost Converter Based on Average-Behavior Circuit Model," *IEEE Transactions on Industry Applications*, vol. 55, no. 2, pp. 1628–1638, mar 2019.

[21] A. V. Rao and K. P. Guruswamy, "Analysis, Design and Simulation of Non-Inverting Buck-Boost DC-DC Converter for Battery Charging," *Proceedings of IEEE International Conference on Disruptive Technologies for Multi-Disciplinary Research and Applications, CENTCON 2021*, pp. 79–84, 2021.

[22] R. V. Munoz, H. Renaudineau, S. Rivera, and S. Kouro, "Evaluation of DC-DC buck-boost partial power converters for EV fast charging application," *IECON Proceedings (Industrial Electronics Conference)*, vol. 2021-Octob, 2021.

[23] W. Shen, T. T. Vo, and A. Kapoor, "Charging algorithms of lithium-ion batteries: An overview," *Proceedings of the 2012 7th IEEE Conference on Industrial Electronics and Applications, ICIEA 2012*, pp. 1567–1572, 2012.

Authorized licensed use limited to: TU Delft Library. Downloaded on September 29,2023 at 08:49:05 UTC from IEEE Xplore. Restrictions apply.